

Supplementary Information

Assembling pore-rich FeP nanorods on the CNT backbone as an advanced electrocatalyst for oxygen evolution

Ya Yan ^{a,b}, Bin Zhao ^a, Sung Chul Yi ^{c,*}, Xin Wang ^{b,*}

^a School of Materials Science & Engineering, University of Shanghai for Science and Technology, 516 Jungong Road, Yangpu District, Shanghai 200093, China

^b School of Chemical and Biomedical Engineering, Nanyang Technological University, 50 Nanyang Avenue, 639798 Singapore

^c Department of Chemical Engineering, Hanyang University, Haengdang-dong, Seongdong-gu, Seoul 133-791, Republic of Korea

* Corresponding authors. E-mail: WangXin@ntu.edu.sg (X.W); scyi@hanyang.ac.kr (S.C.Y.)

Experimental section

Pre-treatment of carbon nanotubes: Carbon nanotubes (CNTs) used in this work are provided by Cnano Technology Limited, of which the diameter is in a range of 20 ~ 60 nm and the length is around several micrometers. 3 g of the CNTs was refluxed in 90 mL of HNO₃ (65 wt. %) at 120 °C for 6 h. After that, the acid treated CNTs were rinsed with DI water until a neutral pH value is reached. Then they were collected by filtration and dried at 60 °C for further use.

Synthesis of the FeO(OH)@CNT hierarchical structure: The growth of α-FeO(OH) nanospindles on CNT backbones was synthesized by a solvothermal method. In a typical procedure, 2 mg of the CNTs was dispersed in the mixture (40 mL) of water and glycerol ($V_{\text{H}_2\text{O}}/V_{\text{C}_3\text{H}_8\text{O}_3} = 3:1$) by ultra-sonication for 30 ~ 60 min. Then 800 mg of ferrous sulfate (FeSO₄·7H₂O, Sigma-Aldrich) was added into the above solution and the mixture was ultrasonicated for another 30 min. Afterward, the above well-dispersed solution was transferred into a 50 mL Teflon-lined stainless steel autoclave, followed by heating at 120 °C for 24 h. Then the autoclave was

naturally cooled to room temperature and the final products are collected by several rinse-centrifugation (2000 rpm) cycles before drying at 60 °C.

Synthesis of the FeP@CNT hierarchical structure: The hierarchical FeP nanorods@CNT nanocomposite was finally fabricated by the pseudomorphic transformation of the FeO(OH)@CNT precursors. Briefly, the FeO(OH)@CNT and NaH₂PO₂ were placed at two separate positions in one closed porcelain crucible with NaH₂PO₂ at the upstream side of the furnace. The weight ratio of the precursor to NaH₂PO₂ is 1:20. Subsequently, the samples were heated at 300 °C for 1 h with a heating speed of 2 °C min⁻¹ in Ar atmosphere. For the control experiment, the CNT supported Fe₂O₃ was prepared by heating the as-prepared FeO(OH)@CNT in air at 400 °C for 4h with a heating speed of 2 °C min⁻¹.

Material Characterization: All transmission electron microscopy (TEM), high-resolution (HR) TEM images, high-angle annular bright-field scanning TEM (BF-STEM) and related energy dispersive X-ray spectroscopy (EDS) were taken from JEOL JEM 2100F at an accelerating voltage of 200 kV. The field emission scanning electron microscopy (FESEM) images were taken on a JEOL JSM 6700F. XRD analysis of different samples was carried out on a X-ray diffractometer (Bruker AXS D8, Cu K λ , λ = 1.5406 Å, 40 kV and 20 mA). X-ray photoelectron spectroscopy (XPS) spectrum was measured on a VG Escalab 250 spectrometer equipped with an Al anode (Al K α = 1846.6 eV). N₂ adsorption/desorption isotherm was conducted to analyze the pore structure. The BET surface area was determined using adsorption data in the relative pressure (P/P_0) range of 0.05-0.25.

Electrochemical measurement: Electrochemical measurements were conducted using an Autolab PGSTAT302 potentiostat (Eco Chemie, Netherlands) at room temperature. A traditional three-electrode cell was used. For polarization and electrolysis measurements, a platinum wire was used as the auxiliary electrode and a double-junction Ag/AgCl (KCl saturated) electrode was used as the reference electrode. The working electrode was prepared on a glass carbon (GC) disk as the substrate. Typically, a mixture containing 3.0 mg catalyst, 2.5 mL ethanol and 0.5 mL Nafion solution (0.05 wt%, Gashub) was ultrasonicated for 15 min to obtain a well-dispersed ink. Then 40 μ L of the catalyst ink (containing 40.0 μ g of catalyst) was loaded onto a glassy carbon electrode of 5 mm in diameter (loading \sim 0.204 mg cm⁻²). The presented current density refers

to the geometric surface area of the glass carbon electrode. The reference electrode is calibrated in the high purity H_2 saturated electrolyte with a Pt wire as the working electrode. All measured potentials vs. Ag/AgCl were converted to a reversible hydrogen electrode (RHE) scale according to the Nernst equation ($E_{\text{RHE}} = E_{\text{Ag/AgCl}} + 0.059 \times \text{pH} + 0.20$) unless stated otherwise. When indicated, measurements were corrected for uncompensated series resistance (R_s). R_s was determined by equating R_s to the minimum impedance between 10 kHz and 1 MHz, where the phase angle was closest to zero.

To characterize FeP@CNT hierarchical structure during the OER process, the catalysts were firstly electrochemically pre-conditioned (30 linear sweep voltammetry (LSV) scans) to reach a stable state. Then the water oxidation activity was measured by LSV with scan rate of 5 mV s^{-1} in 1.0 M KOH. Commercial IrO_2 catalyst was also measured for reference. For the stability test, galvanostatic experiment was performed in 1.0 M KOH at 25°C applying a fixed current density (10 mA cm^{-2}) to the pretreated working electrode for 14 hours. During the measurement, the working electrodes were mounted at a rotating disc electrode with a rotating rate of 1600 rpm during the test and a flow of O_2 was maintained over the electrolyte (1.0 M KOH) during electrochemical measurements in order to ensure the $\text{O}_2/\text{H}_2\text{O}$ equilibrium. The overpotential was calculated as follows: $\eta = E (\text{vs. RHE}) - 1.23$, considering $\text{O}_2/\text{H}_2\text{O}$ equilibrium at 1.23 V vs. RHE.

Faraday efficiency was estimated using volumetric method. The actual-evolved oxygen gas on FeP@CNT electrode was collected in a 50 ml graduated tube, which was filled with the electrolyte. The time points at each 0.5 ml of collected gaseous were recorded. Meanwhile, the accumulated charges passing through the working electrode were recorded using electrochemical workstation at the overpotential of 370 mV for oxygen gas for 120 min. The quantity of oxygen produced during this time was determined by converting its volume to mole using the ideal gas law. The faradaic yield was calculated from the total amount of charge passed through the cell and the total amount of oxygen produced, assuming that four electrons are needed to produce one O_2 molecule.

The electrocatalytic HER performance were tested in a H_2 -saturated 1.0 M KOH electrolyte. Prior recording the HER activity of catalysts, the as-prepared electrodes were activated by 10 LSV scans along the potential window of $-1.20 \sim -1.8 \text{ V vs. RHE}$ in 1.0 M KOH at a scan rate of 50 mV s^{-1} . And then steady-state LSV were

performed and recorded at scan rate of 5 mV s^{-1} . Commercial Pt/C catalyst was also measured for reference. During the measurement, the working electrodes were mounted at a rotating disc electrode with a rotating rate of 1600 rpm.

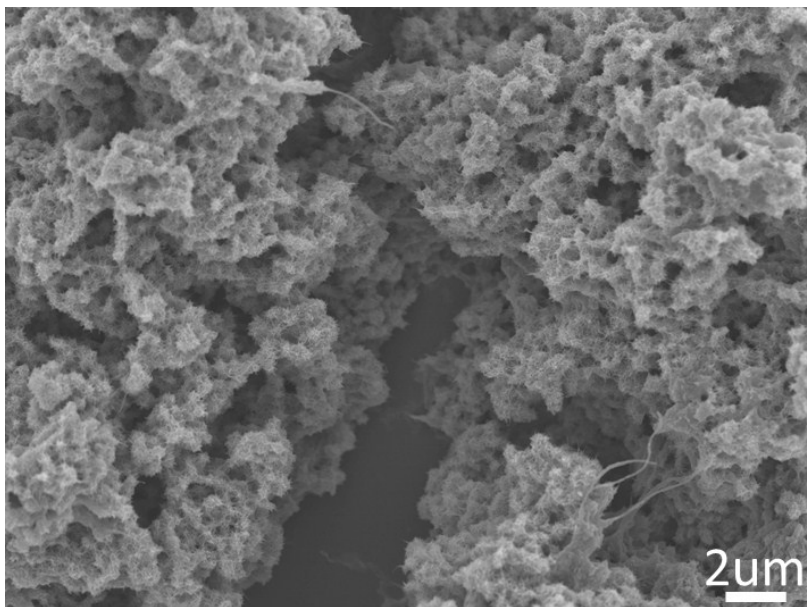


Fig. S1 Low magnification SEM image of FeO(OH)@CNT.

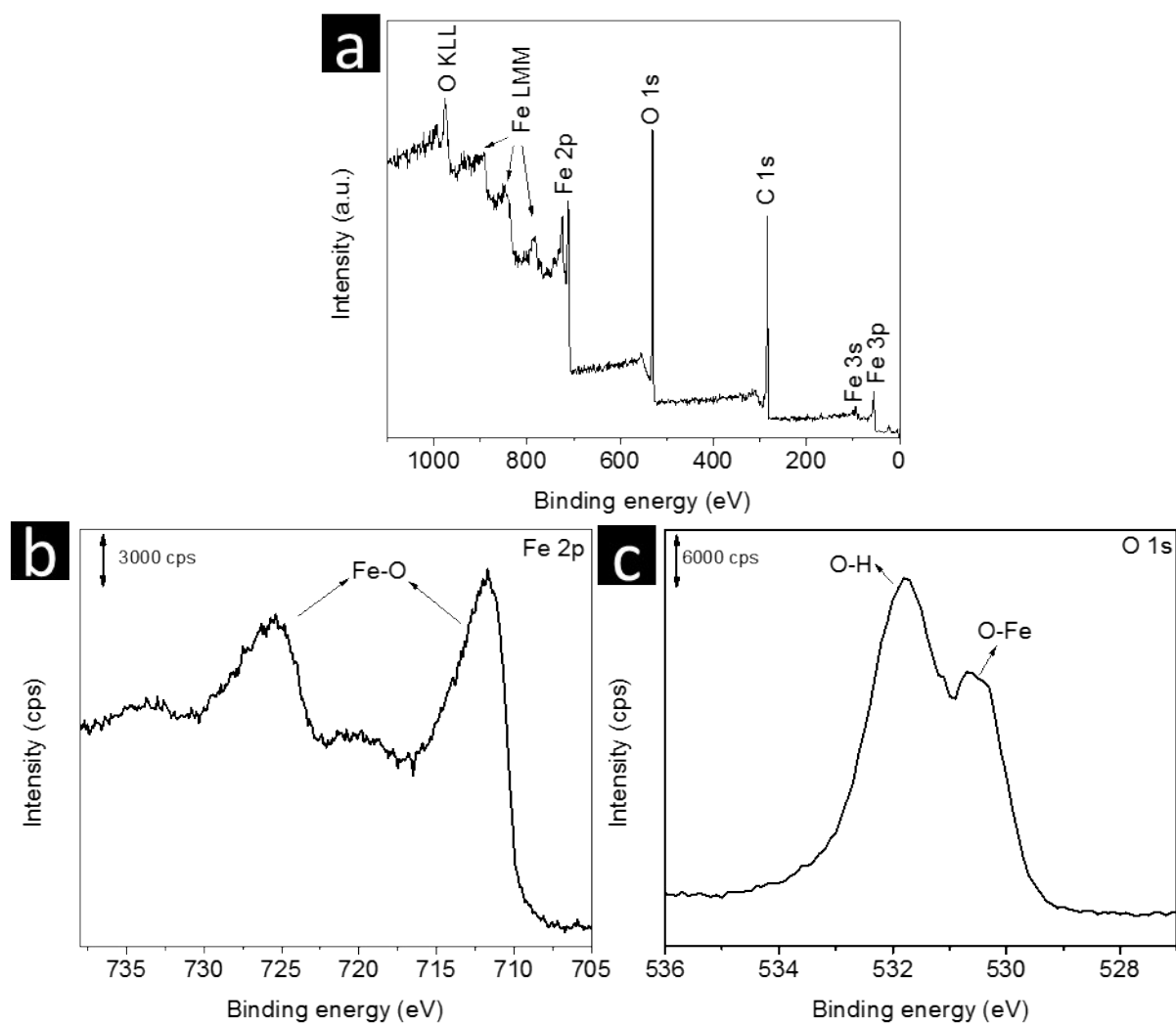


Fig. S2 (a) XPS survey spectra and (b-c) high-resolution XPS spectra of FeO(OH)@CNT precursor.

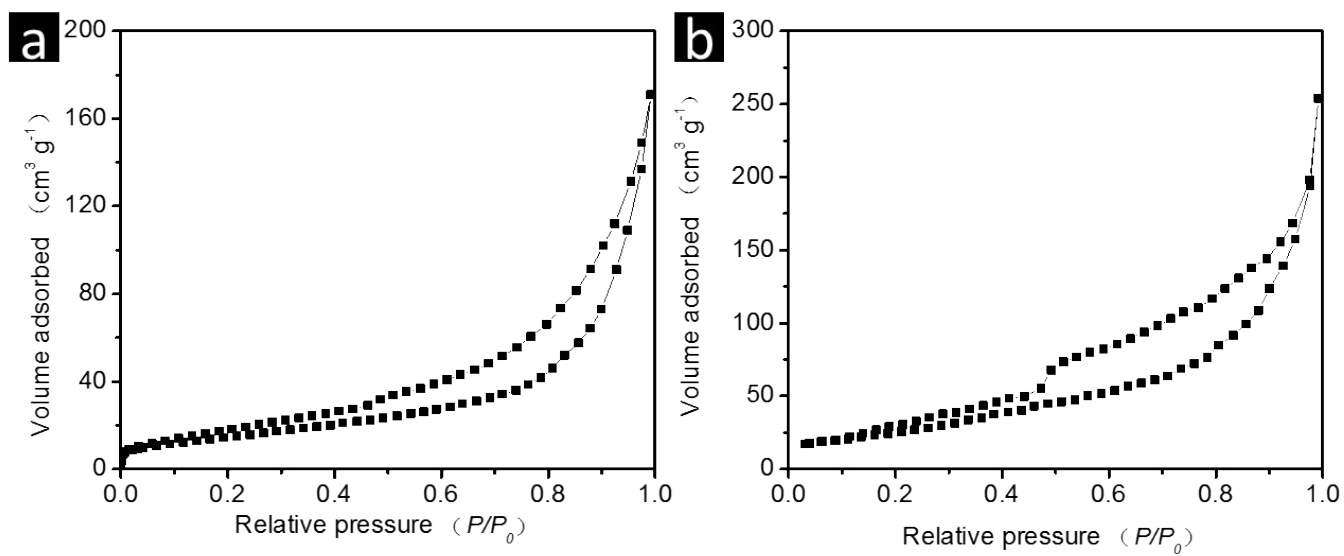


Fig. S3 N₂ adsorption/desorption isotherms of (a) FeO(OH)@CNT and (b) FeP@CNT hierarchical structures.

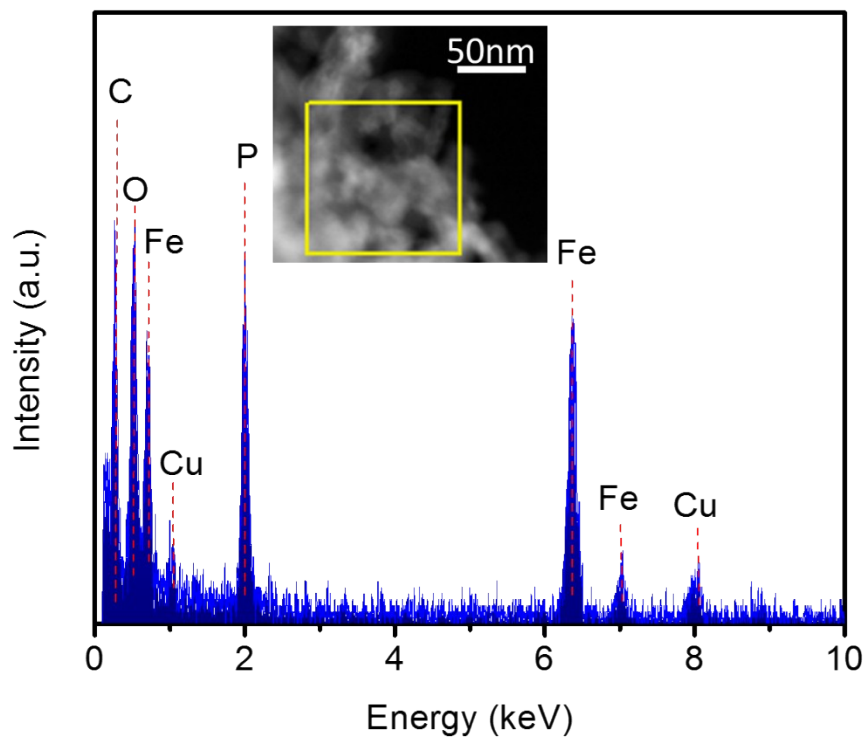


Fig. S4 EDS spectrum of FeP@/CNT obtained under scanning TEM (STEM) mode (the Cu peaks arise from the Cu mesh).

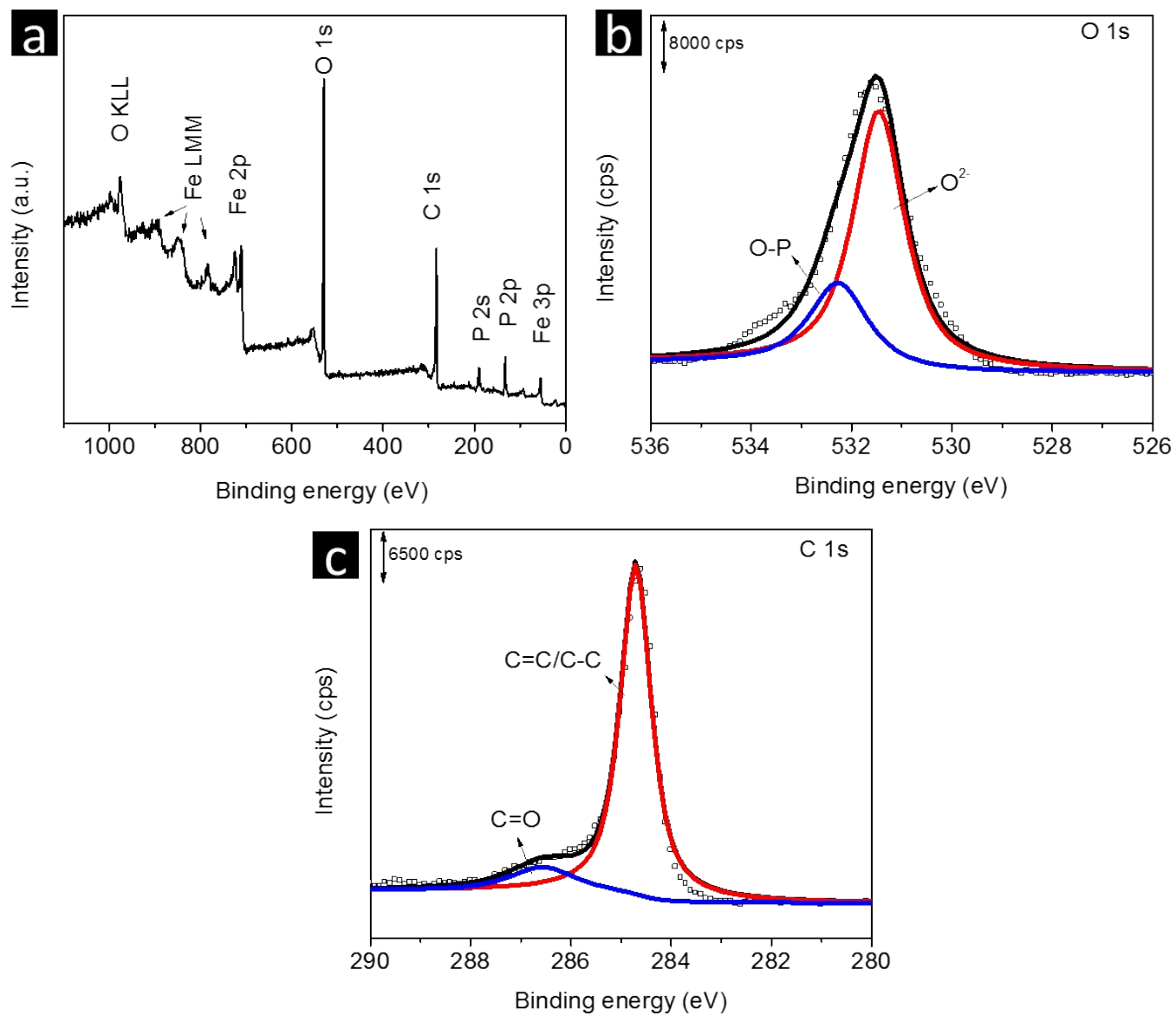


Fig. S5 (a) XPS survey spectra and (b-c) high-resolution XPS spectra of FeP@CNT hybrid material.

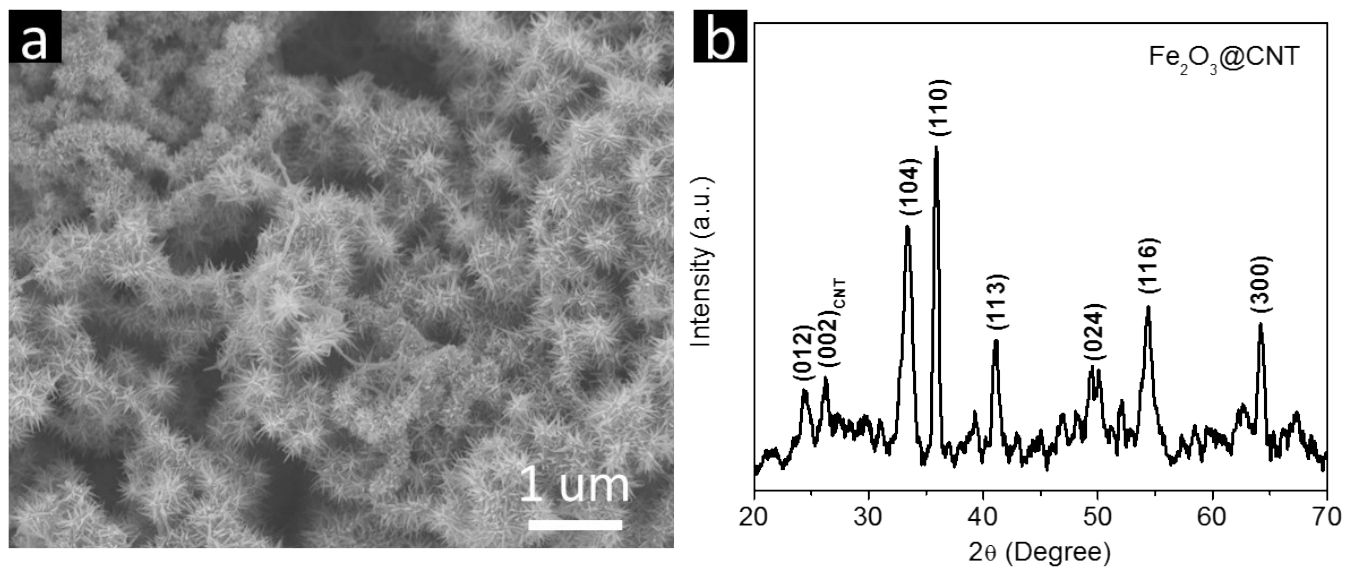


Fig. S6 SEM image (a) and XRD pattern (b) of $\text{Fe}_2\text{O}_3@\text{CNT}$.

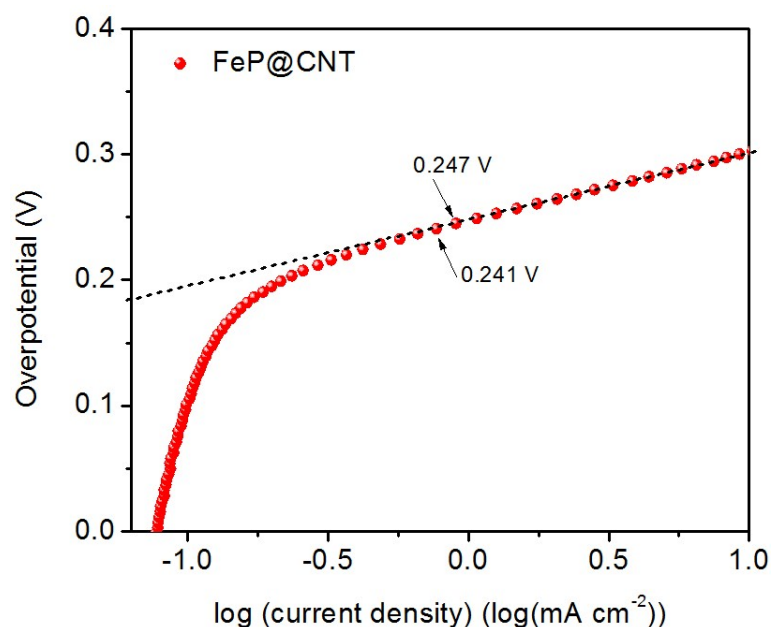


Fig. S7 The Tafel plot of FeP@/CNT hierarchical structure in the region of low current densities.

The onset potential for HER was read from the semi-log (Tafel) plot. For example, the semi-log plot of FeP@/CNT hierarchical structure in the region of low current densities as displayed in **Fig.S6** shows a linear relationship below -0.247V but starts to deviate above -0.241V. Therefore, -0.247 was chosen as the onset potential for FeP@/CNT hierarchical structure. The same method was applied on determining the overpotential for other samples.

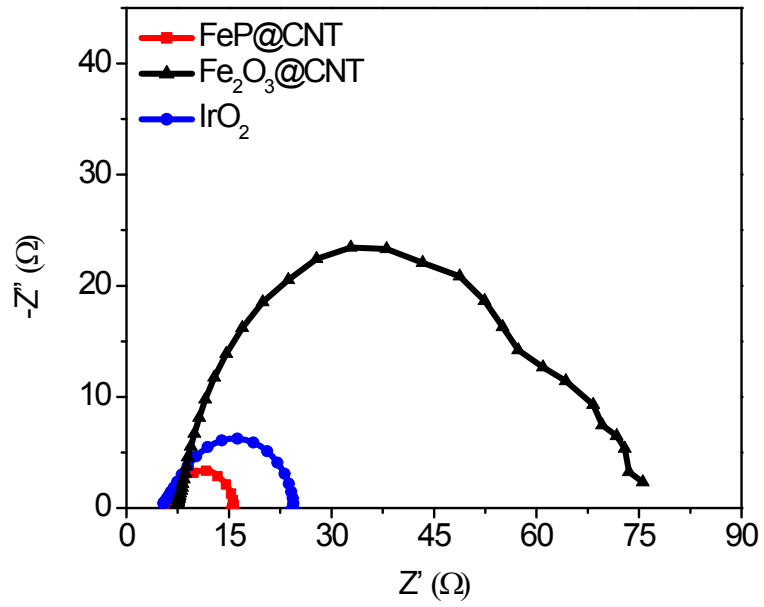


Fig. S8 Nyquist plots of the tested samples. Z' is the real impedance and $-Z''$ is the imaginary impedance. The high-frequency intercept of the semicircle on the real axis is assigned to the ohmic series resistance (R_s). iR correction with the series resistance (R_s) is performed by $\eta_{\text{corr}} = \eta - jR_s$.

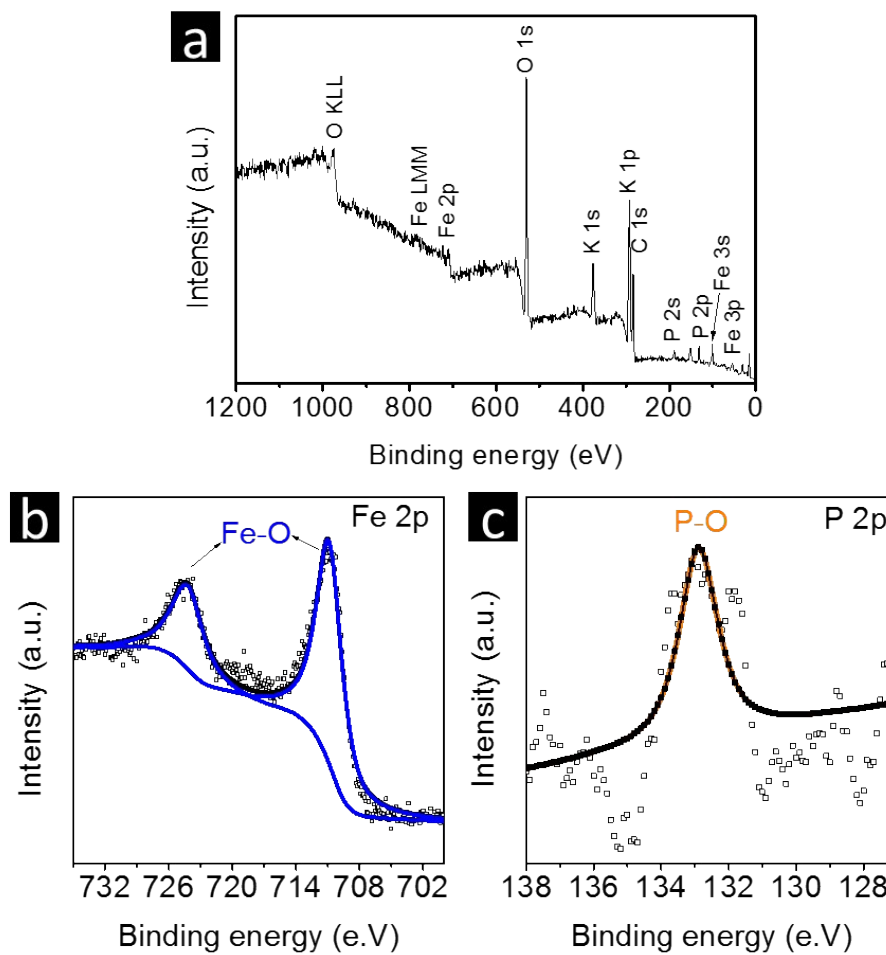


Fig. S9 XPS survey (a) and Fe 2p (b) and P 2p (c) spectra of the FeP@/CNT catalyst after the OER in 1.0 M KOH.

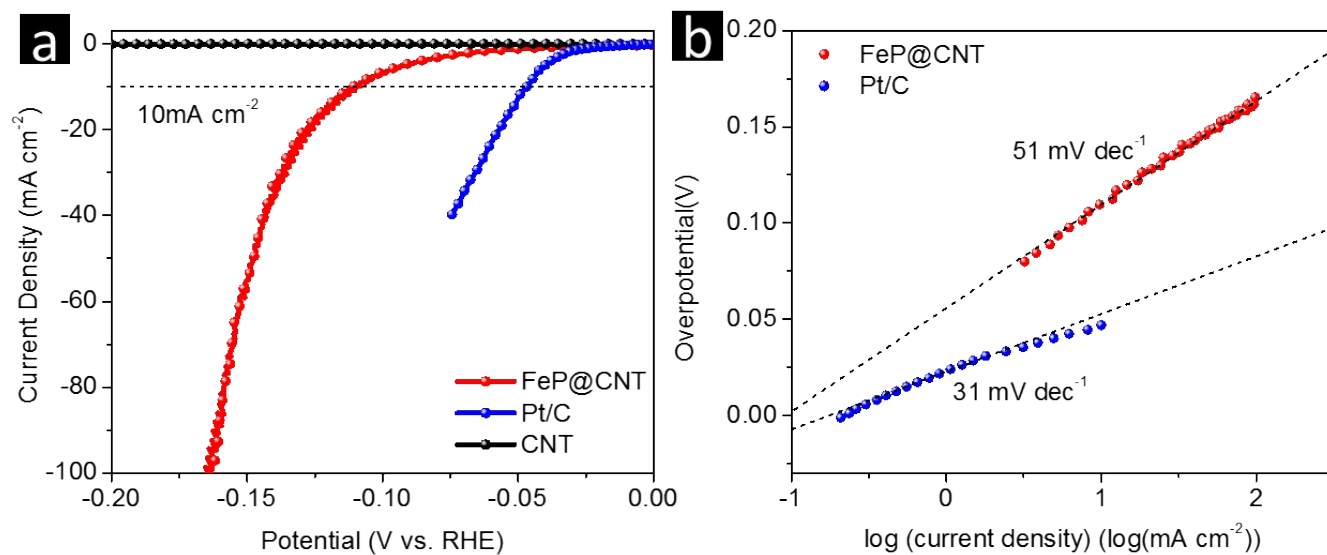


Fig. S10 (a) *i*R-corrected HER polarization curves and (b) corresponding Tafel plots measured in 1.0 M KOH.

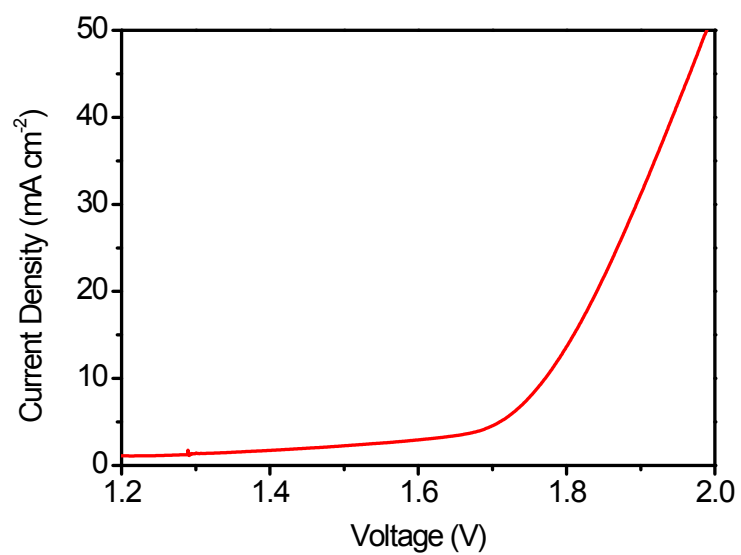


Fig. S11 Current-potential response (anode current) of a two-electrode alkaline electrolyzer composed of FeP@/CNT bifunctional catalysts.

Table S1. OER activities of the FeP@CNT and reported catalysts in alkaline condition.

Catalysts	Electrolyte	η_{ons} et (mV)	Tafel slope (mV dec ⁻¹)	j_{geo} (mA cm ⁻²)	Loading mass (mg cm ⁻²)	Ref.
FeP@CNT	1.0 M KOH	250	53	10 @η= 300 mV	0.2	This work
RuO ₂	0.1M KOH	-	-	10 @ η = 298 mV	-	J. Phys. Chem. Lett. 2012, 3, 399
IrO ₂		-	-	10 @ η = 288 mV		
(Co _{0.54} Fe _{0.46}) ₂ P	1.0 M KOH	-	-	10 @ η = 280 mV	-	Angew. Chem. Int. Ed. 2015, 54, 9642
Co-P film	1.0 M KOH	-	47	10 @ η = 345 mV	Co=2.52 P=0.19	Angew. Chem. Int. Ed. 2015, 54, 6251
Porous Co phosphide/Co phosphate thin film	1.0 M KOH	220	65	30 @ η = 330 mV	0.1	Adv. Mater., 2015, 27, 3175
N ₂ P nanoparticles	1.0 M KOH	-	47	10 @ η = 290 mV	0.14	Energy Environ. Sci. 2015, 8, 2347.
Ni-P porous nanoplates	1.0 M KOH	250	64	10 @ η = 300 mV	0.2	Energy Environ. Sci. doi: 10.1039/C6EE00100A
De-LNiFeP/rGO	1.0 M KOH	240	33.6	10 @ η = 258 mV	0.5	Energy Environ. Sci., 2015,8, 1719
Fe-Ni oxides	1.0 M KOH	-	51	10 @ η >375mV	1	ACS Catal. 2012, 2, 1793
NiFeOx film	1.0 M NaOH	-	-	10 @ η >350 mV	-	J.Am.Chem.Soc. 2013, 135, 16977
Ni-Fe LDH/CNT	1.0 M KOH	220	31	5 @ η = 288 mV	0.25	J. Am. Chem. Soc. 2013, 135, 8452
FeNi-rGO LDH	1.0 M KOH	210	39	10 @ η = 210 mV	0.25	Angew. Chem. Int. Ed. 2014, 53, 7584
NiFe LDH nanosheets	1.0 M KOH	-	40	10 @ η = 300 mV	1	Nat. Commun. 2014, 5, 4477
amorphous Fe-Ni oxides nanospheres	1.0 M KOH	-	48	10 @ η = 286 mV	0.1	Angew. Chem. Int. Ed. 2014, 53, 7547
Ni ₃₀ Fe ₇ Co ₂₀ Ce ₄₃ O _x	1.0 M NaOH	270	70	10 @ η = 310 mV	-	Energy Environ. Sci. 2014,7, 682
Amorphous Ni-Co Oxide	1.0 M NaOH	250	39	10 @ η = 325 mV	-	ACS Nano, 2014, 8, 9518
NiCo _{2.7} (OH) _x amorphous nanocages	1.0 M KOH	250	67	10 @ η = 350 mV	0.2	Adv. Energy Mater. 2015, 5, 1401880

Table S2. HER activities of the FeP@CNT and reported catalysts in alkaline condition.

Catalysts	Electrolyte	η_{onset} (mV)	Tafel slope (mV dec ⁻¹)	j_{geo} (mA cm ⁻²)	Loading mass (mg cm ⁻²)	Ref.
FeP@CNT	1.0 M KOH	-	51	10 @ η = 110 mV	0.2	This work
FeP NAs/CC	1.0 M KOH	86	146	10 @ η = 218 mV	1.5	ACS Catal., 2014, 4, 4065
Co _{0.59} Fe _{0.41} P	1.0 M KOH	39	72	10 @ η = 92 mV	0.35	Nanoscale, 2015, 7, 11055
Ni ₅ P ₄ (pellet)	1.0 M NaOH	-	98	10 @ η = 49 mV	50mg in 6mm pellet	Energy Environ. Sci. 2015,8, 1027
Ni ₂ P(pellet)	1.0 M NaOH	-	118	10 @ η = 69 mV		
MoP	1.0 M KOH	-	48	-	0.86	Energy Environ. Sci. 2014, 7, 2624
Porous Co phosphide/Co phosphate thin film	1.0 M KOH	-	-	30 @ η = 430 mV	0.1	Adv. Mater., 2015, 27, 3175
Co-P film	1.0 M KOH	-	42	10 @ η = 94 mV	Co=2.52 P=0.19	Angew. Chem. Int. Ed. 2015, 54, 6251
Ni _{0.33} Co _{0.67} S ₂	1.0 M KOH	50	118	10 @ η = 88 mV	0.3	Adv. Energy Mater. 2015, 5, 1402031